



Published in final edited form as:

Xenotransplantation. 2013 ; 20(5): 277–291. doi:10.1111/xen.12047.

N-linked glycan profiling of GGTA1/CMAH knockout pigs identifies new potential carbohydrate xenoantigens

Christopher Burlak^{1,2}, Marshall Bern³, Alejandro E. Brito³, Dragan Isailovic⁴, Zheng-Yu Wang², Jose L. Estrada², Ping Li², and A. Joseph Tector²

²Department of Surgery, Indiana University School of Medicine, 635 Barnhill Dr., MS B-008, Indianapolis, IN 46202

³Palo Alto Research Center, 3333 Coyote Hill Road, Palo Alto, CA 94304, USA

⁴Department of Chemistry, University of Toledo, 2801 W. Bancroft St., Toledo, OH 43606, United States

Abstract

Background—The temporary or long-term xenotransplantation of pig organs into people would save thousands of lives each year if not for the robust human antibody response to pig carbohydrates. Genetically engineered pigs deficient in galactose α 1,3 galactose (gene modified: GGTA1) and N-glycolylneuraminic acid (gene modified: CMAH) have significantly improved cell survival when challenged by human antibody and complement *in vitro*. There remains, however, a significant portion of human antibody binding.

Methods—To uncover additional xenoantigens we compared the asparagine-linked (N-linked) glycome from serum proteins of humans, domestic pigs, GGTA1 knockout pigs and GGTA1/CMAH knockout pigs using mass spectrometry. Carbohydrate structures were determined with assistance from GlycoWorkbench, Cartoonist, and SimGlycan software by comparison to existing database entries and collision-induced dissociation fragmentation data.

Results—Matrix-assisted laser desorption/ionization time-of-flight mass spectrometry (MALDI-TOF-MS) analysis of reduced and solid-phase permethylated glycans resulted in the detection of high mannose, hybrid, and complex type N-linked glycans in the 1000 to 4500 m/z ion range. GGTA1/CMAH knockout pig samples had increased relative amounts of high-mannose, incomplete and xylosylated N-linked glycans. All pig samples had significantly higher amounts of core and possibly antennae fucosylation.

¹Address Correspondence to: Christopher Burlak PhD, Cburlak@iupui.edu, office 317-274-3244, fax 317-274-7429.

Author Contributions:

Christopher Burlak- Concept/design, Data analysis/interpretation, Data collection, Drafting article and Statistics.

Marshall Bern and Alejandro Brito- Software design and Critical review of article.

Dragan Isailovic- Data interpretation and Critical review of article.

Zheng-Yu Wang- Assisted with data collection and Critical review of article.

Ping Li- Production of genetically modified pig cells.

Jose Estrada- Production of genetically modified pigs by somatic cell nuclear transfer and In vitro fertilization and Critical review of article.

A. Joseph Tector- Critical review of article, Approval of article and Secured Funding.

Conclusions—We provide for the first time a comparison of the serum protein glycomes of the human, domestic pig and genetically modified pigs important to xenotransplantation.

Keywords

MALDI-TOF/TOF; asparagine-linked; glycome; permethylation; serum; xenotransplantation

INTRODUCTION

Xenotransplantation of pig organs to humans is a potential solution to the human organ shortage. Pig xenografts are rejected, however, by human antibody binding to pig antigens followed by complement fixation and cell lysis; called antibody-mediated rejection (AMR). The most prominent antigen identified thus far is the oligosaccharide galactose- α -1,3 galactose (aGal) (1,2). Genetic alteration of the α -1,3-galactosyl transferase gene that catalyzes the synthesis of aGal yielded a knockout pig with delayed AMR during transplantation to immunosuppressed non-human primates (3).

The second major barrier to using pig organs in xenotransplantation is the presence of the N-glycolyl neuraminic acid (neu5Gc) in pigs. The addition of a glycolyl group to N-acetyl neuraminic acid (neu5Ac) is mediated by the enzyme cytidine monophosphate-N-acetylneuraminic acid hydroxylase (CMAH). The production of Neu5Gc is absent in humans due to a mutation in the CMAH gene. Like aGal, the absence of neu5Gc in humans during immunologic education has resulted in the presence of IgG and IgM antibody that bind to these carbohydrate antigens and fix complement (4–6). We have recently produced a pig using zinc-finger endonucleases and somatic cell nuclear transfer that lacks production of the aGal and neu5Gc epitopes (4). Cells from the GGTA1/CMAH knockout pigs are bound by less antibody (IgG and IgM) and are rejected less vigorously by a complement-based assay designed to estimate AMR (4). There remains, however, human IgG and IgM that bind to the GGTA1/CMAH knockout pig cells.

An analysis of the carbohydrate targets of human antibodies by carbohydrate microarray found aGal to be immune-reactive, but not the most immune-reactive glycan target (7). Interestingly, rhamnose, galactose-x-galactose and β 1,4 linked mannose bound more antibody than aGal. With so many human antibodies directed towards carbohydrate targets present in the serum of healthy individuals it seems likely that the GGTA1/CMAH knockout pigs may bear additional carbohydrate epitopes that could be genetically modified to benefit xenotransplantation.

Matrix-assisted laser desorption/ionization (MALDI) followed by one or two time of flight (TOF) stages of mass spectrometry analysis is a very sensitive technique that can be used to determine the mass-to-charge ratios (m/z) of ions in simple or complex samples. This technology has been used effectively to uncover differences among healthy people and those with cancer by measuring changes to the N-linked glycans harvested from serum proteins (8,9). Changes to the N-linked glycans correlated to those patients in whom disease had progressed. The N-linked glycans of serum proteins have been representative of glycan changes in organs important to xenotransplantation (10). In fact most serum glycoproteins originate from the liver (11,12). This suggests that serum glycoproteins may represent a

readily available and efficient source for human and pig glycans. MALDI-TOF/TOF has also been used to define the composition of N-linked glycans present on human embryonic stem cells and human innate immune cells (8,13). The MALDI-TOF and TOF/TOF of native branched and sialylated acidic glycans can be improved by conversion to their methylated derivatives. Reduced and permethylated N-linked glycans ionize more efficiently than native glycans and give more detailed structural data when fragmented by collision-induced dissociation (9,14,15). These modifications can be carried out with as little as 1 µl of serum facilitating the processing of multiple samples simultaneously on micro scale (9).

In this study we reduced and permethylated the N-linked glycans of serum proteins from humans, domestic pigs, GGTA1 knockout pigs and GGTA1/CMAH knockout pigs. Modified glycans were analyzed in positive ion mode using a MALDI-TOF/TOF mass spectrometer (Figure 1). We determined that the serum N-linked glycomes of humans and pigs are reproducible and highly diverse. The data demonstrated the presence of known xenoantigens in domestic pigs and highlighted several differences between the glycans of humans, domestic and genetically modified pigs.

MATERIALS AND METHODS

Materials

The enzyme PNGase F, detergents, liquid chemical reagents, sodium hydroxide beads and high pressure liquid chromatography (HPLC) grade water were purchased from Sigma Chemical Co. (St. Louis, MO). Empty microspin columns were purchased from Harvard Apparatus (Holliston, MA) and graphitized carbon column for glycan purification were from Y-Carbon (Norristown, PA). The MALDI matrix, 2,5-dihydroxybenzoic acid, was purchased from Protea Biosciences (Morgantown, WV).

Serum samples

Blood samples were collected from healthy humans of blood type A, Landrace predominant mix breed pigs, GGTA1 knockout pigs, or GGTA1/CMAH knockout pigs using Institutional Review Board and Institutional Animal Care and Use Committee approved protocols (IRB #0808-60 and IACUC# 10345) (Figure 1A). Blood was collected into sterile non-heparinized Vacutainer tubes and allowed to clot for 30 minutes at room temperature. The upper serum layer was collected, cleared by centrifuged, and stored at -80 °C until use.

Purification of N-linked glycans

Human or pig serum proteins (200 µL of serum) were diluted to 800 µL with a 10 mM sodium phosphate (pH = 7.5) containing 0.1% β-mercaptoethanol, and 0.1% SDS and incubated at 60 °C for 60 min. The N-linked glycans were enzymatically cut from the denatured and reduced proteins using 5 mU of PNGase F and incubating the samples for 24 h at 37 °C (Figure 1B). The released glycans were purified by removing deglycosylated proteins on graphitized carbon columns. The graphitized carbon was activated with three 1 mL aliquots of 85% acetonitrile (ACN)/15% H₂O/0.1% trifluoroacetic acid (TFA) (solution A), and equilibrated with three 1 mL aliquots of 5% ACN/95% H₂O/0.1% TFA (solution B). The samples were diluted to 4 mL with solution B, then loaded onto the graphitized

carbon column, collected by centrifugation, and reapplied to the same material a total of 3 times. The column was washed 6 times with 5-mL solution B. Glycans were eluted using three 1 mL aliquots of a solution A. Each sample was then fractionated into 4 equal aliquots and dried using a vacuum centrifuge. Completely dried glycans were resuspended in 1ml of 10mg/ml ammonia-borane complex made with HPLC grade H₂O and heated to 60°C for 60 minutes. Samples were cooled to room temperature, excess ammonia-borane complex was disrupted by the addition of three 200 µL aliquots of glacial acetic acid, added over a 3 h time period with mixing. After drying by vacuum centrifugation, borate salts were evolved as their methyl esters by the addition of three 1 mL aliquots of HPLC grade methanol, followed by drying vacuum centrifuge between additions.

Solid-phase extraction and reduction

The N-linked glycans from each analysis were permethylated statically following the protocol of Mechref et al and Alley et al. (9,15) in N,N-dimethylformamide (DMF) (Figure 1C). Briefly, spin-columns were filled with sodium hydroxide beads suspended in ACN. The spin columns were washed 3 times with 1 mL DMF. Dried glycan samples were resuspended in 250 µL DMF, 90 µL methyl iodide, and 18 µL H₂O. Samples were then applied to individual spin columns and incubated for 15 min at room temperature. Samples were collected by centrifuged at low speed, 90 µL of methyl iodide was added and re-applied to the spin column for an additional 15 minutes and collected by centrifugation. Spin columns were rinsed with 500 µL ACN and added to samples. Permethylated glycans were recovered by a 4 mL chloroform extraction and washed by inversion with 4 mL 0.5 M NaCl solution in HPLC-grade water. Following the extraction, the chloroform layer was divided into 4 aliquots and dried in a vacuum centrifuge. Dried, reduced, and permethylated glycans were used immediately or stored at -80°C.

MALDI TOF/TOF analysis

Prior to MALDI-TOF analysis, the samples were reconstituted in a 40 µL 0.2% TFA in HPLC grade H₂O. Graphitized carbon pipet tips (Sigma Chemical Co., St. Louis, MO) were activated and equilibrated as described above for columns. Glycans were eluted three times from graphitized carbon pipet tips with 0.5 µL 90% methanol and 10% H₂O sequentially onto a stainless steel MALDI plate prespotted with 0.5 µL 10 mg/mL 2,5-dihydroxybenzoic acid in a 50% H₂O, 50% methanol solution and 1 mM sodium acetate (to promote sodium adduct formation) with spot drying between elutions. A final elution with 0.5 µL of 100% ACN was layered onto each dry sample spot. Samples were spotted in duplicate. The samples were investigated manually using an Applied Biosystems Sciex 5800 MALDI-TOF/TOF mass spectrometer (Framingham, MA) in positive-ion mode, with a ion range of 1000 to 5000 m/z with a focus of 2500 m/z. A total of 5000 laser shots were acquired for each sample spot. Mass spectra were baseline corrected, noise removal applied, and peak analyzed with Data Explorer software (AB Sciex, Framingham, MA).

Structural determination

Mass spectra were annotated with GlycoWorkbench software (16), Cartoonist MS/MS2 (Palo Alto Research Center, Palo Alto, CA,(17)) and SimGlycan v4 (Premier Biosoft, Palo Alto, CA) following the manufacturers tutorials or suggestions and using the nomenclature

proposed by the Consortium for Functional Glycomics (18). Briefly, T2D or Txt files were opened in the software and peaks were searched by all available databases. Structural annotations were species matched and considered potentially correct annotations. MALDI-TOF/TOF mass spectra were opened in GlycoWorkbench and peaks were annotated with all possible structures for a given ion. The MALDI-TOF annotation was used as a guide to determine the possible fragment ions observed in MALDI-TOF/TOF analysis. Final annotations (Figures 3 and 4) were based on a combination of MALDI-TOF and TOF TOF mass spectra and assistance from all three softwares. The MALDI-TOF/TOF annotations used the nomenclature proposed by Domon and Costello (19) without cross ring fragmentation (Figure 1D).

Statistical analysis

Paired one-tailed T-test with Graphpad Prism software (GraphPad Software Inc., La Jolla, CA) were used to determine the significance percent relative intensity differences between human and pig samples. Significance was $p < 0.05$ where indicated (Figure 6). The percent relative intensity was calculated from each spectral intensity normalized to the most abundant mass in that spectra set to 100 percent.

RESULTS

Serum protein glycome

The major surface antigens of pig cells in regards to xenotransplantation have been carbohydrates. The N-linked glycans of serum proteins are a reflection of organism-wide glycosylation patterns and are a plentiful source of carbohydrates from both humans and pigs. Asparagine linked glycans from humans, domestic pigs, GGTA1 knockout pigs and GGTA1/CMAH knockout pigs were removed by PNGaseF and isolated by selective retention and elution from graphitized carbon columns. This technique irreversibly bound the sample protein and allowed elution of free N-linked glycans. Glycans were stabilized by reduction and permethylation enabling the consistent collection of whole ion and fragmented ion mass spectra. Complete permethylation was verified by the absence of partially-permethyated -14 Da ions preceding the most abundant ions in the spectra. This is demonstrated by the absence of ion 1581.8 m/z 14 Da downstream of ion 1595.8 m/z , Man5 (Figure 2 black arrow). The ions derived from MALDI-TOF analysis were singly charged and sodiated ($[M + Na]^+$). Although no potassium was included in matrix or sample buffer it is possible that $[M + K]^+$ could occur as a contaminant during permethylation. Electro spray ionization often gives rise to K adducts but MALDI using the matrix 2,5-dihydroxybenzoic acid in the presence of 1 mM sodium acetate typically creates $[M + Na]^+$ adducts. Never the less, we investigated the Man5 peak for a $+16$ Da ion that would be indicative of a K adduct instead of Na adduct and did not find one (Figure 2 grey arrow). It is possible, however, that non-sialylated glycans form adducts differently than sialylated glycans. We looked for an upstream $+16$ Da ion from sialylated glycans and found that in human samples 2808.3 and 3237.7 m/z had $+16$ Da ions upstream while ions 2447.1 , 3257.6 and 3792.9 m/z had ions $+17$ or $+18$ Da upstream. If potassium adducts were present in our samples we would expect them to be more consistent and therefore all of the structures assigned were sodiated. Tentative glycan structures were derived from database searches using GlycoWorkbench

(16), Cartoonist (17) and SimGlycan (20). MALDI-TOF/TOF fragmentation ion patterns were analyzed manually and with GlycoWorkbench software to verify potential glycan structures (16). The N-linked glycan analysis was divided into low range (1000 to 3100 m/z) and high range (3100 to 4500 m/z) spectra due to relative difference in spectral intensity. The glycan structures shown are correct in composition and antennae but may have positional isomers of sialylation or fucosylation that cannot be accounted for with the current technology.

Human serum protein glycome

MALDI-TOF/TOF analysis resulted in the assignment of 39 human glycan structures (Figures 3A and 4A). Low range spectra ($n=3$) were predominantly composed of ion 2808.3 m/z annotated as hex5,hexNAc4,neuAc2 a bi-antennary N-linked glycan without core fucosylation (Figure 3A). High range spectra ($n=3$) were predominantly composed of ion 3618.8 annotated as hex6,hexNAc5,neuAc3 a triantennary N-linked glycan without core fucosylation (Figure 4A). Mass spectra of human samples contained a minority of mannosylated core glycans and truncated N-linked glycans or partial synthesis products by comparison. Peak ion 2808.3 was found in pig and human samples. Peak ion 3618.8 was unique to the human glycan samples. High range glycans were more prevalent in the human samples and contained complex tri and tetra antennary structures. The ions 3564.1 (hex6,hexNAc5,dhex1,neuGc2), 3708.6 (hex5,hexNAc5,neuGc3) and 4432 (hex8,hexNAc8,neuAc1,neuGc1) were suggested to contain terminal neu5Gc and was supported by MALDI-TOF (Figure 4A) and TOF/TOF fragmentation analysis (not shown). High mass glycans were more prevalent in all human samples. There were no significant differences in sialylation patterns between humans and pigs for the annotated glycans (Figure 3 and 4). High mass glycans among humans and pigs were observed to contain up to 3 neuAc saccharides (3792.9 m/z human Figure 4A). These comparisons were made without bias for the structures we expected to see absent from the genetically modified pigs. There is the potential for blood group or unique antigens to occur as a heterogeneous population of glycans but this technology cannot differentiate those structures from a single mass. Therefore, annotation was based on the most abundant peaks in the fragmentation spectra and those most prevalent in the available databases. Fragmentation data suggest that more than one sialic acid on any bi-antennary glycan could be in series or parallel on antennae as indicated by fragment ions 344.2 [H^+] annotated as Z-neuAc-B and 376.2 [H^+] annotated as neuAc-B (Figure 5D). Thus annotations with more than one neuAc should be considered variable as depicted in Figures 3 and 5.

Porcine serum protein glycome

MALDI-TOF/TOF fragmentation analysis resulted in the assignment of 37 domestic pig, 36 GGTA1 knock out pig and 34 GGTA1/CMAH knockout pig glycan structures (Figures 3B, C, D and 4B, C, D). The domestic and genetically modified pigs produced similar glycan profiles. Overall, mannosylated glycans were more prevalent in the pig samples as compared to humans. Ion 1362.7 (hex3,hexNAc2,dhex1) annotated as a core fucosylated N-linked glycan, was only present in pig samples and more abundant in genetically modified pigs. Ion 1595.6 (hex5,hexNAc2) a core N-linked glycan bearing 5 mannose saccharides (Man5) was present in humans but increased significantly from domestic pigs to the GGTA1/CMAH

knock out pigs (n=3, P<0.05) (Figure 3 and 6). Fragmentation of ion 1595.6 gave rise to ions 187 [H⁺], 316.2 [Na⁺], 490.3 [Na⁺], 839.5 [Na⁺], 1075.7 [Na⁺], 1302.7 [Na⁺], and 1377.6 [Na⁺] that corresponded to the proposed structure (Figure 5A). The other high-mannose containing glycans, Man6 and Man7, were more abundant in pigs than human samples. These findings excluded Man9, which appeared equally present in human and genetically modified pig samples (Figure 3 and Table 1).

Pig samples had an accumulation of incomplete or truncated glycans as indicated by ions 1677.7 (hex3,hexNAc4), annotated as an N-linked glycan, 1851.8 (hex3,hexNAc4,dhex1) a fucosylated N-linked glycan and 2055.8 (hex4,hexNAc4,dhex1) annotated as a fucosylated N-linked glycan with a single terminal galactosylation (Figure 3 B, C and D). Fragmentation of ion 1851.7 gave rise to ions 260.1 [H⁺], 490.3 [Na⁺], 676.3 [Na⁺], 921.4 [Na⁺], 1125.5 [Na⁺], 1384.6 [Na⁺], and 1592.8 [Na⁺] that corresponded to the proposed structure (Figure 5B).

Ion 2245.8 (hex5,hexNAc4,pen1) was annotated as an N-linked glycan structure with a core xylose and present in human and pig samples (Figure 3). Ion 2245.8 was present in only 1 of the human samples and appeared to increase in relative intensity with genetic modifications in pigs (n=3, P<0.05) (Figure 5C). Fragmentation of ion 2245.8 gave rise to ions 187 [H⁺], 197 [Na⁺], 472.2 [Na⁺], 490.3 [Na⁺], 866.5 [Na⁺], 1316.6 [Na⁺], 1764.8 [Na⁺], 1779 [Na⁺], 1783.1 [Na⁺] and 1796.8 [Na⁺] corresponded to the proposed structure (Figure 5C). We cannot determine the actual position of xylose due to isomerism but based on fragmentation data and existing database entries a beta-1,2 linkage (from plants) to a core mannose was shown.

The ions 2621.2 (hex5,hexNAc4,dhex1,neuAc1) and 2982.2 (hex5,hexNAc4,dhex1,neuAc2) were two of the most prevalent in pig samples. Ion 2621.2 and 2982.2 were minority peaks in human samples and corresponded to non-fucosylated structures which were the most prevalent low mass peaks in human samples (Figure 3). Ion 2982.2, the core fucosylated version of ion 2808.2 (hex5,hexNAc4,neuAc2), was significantly more abundant in all of the pig samples as compared to humans (n=3, P<0.05) (Figure 5D). Fragmentation of ion 2982.2 gave rise to ions 376.2 [H⁺], 490.3 [Na⁺], 847.4 [Na⁺], 1333.8 [Na⁺], 1691.0 [Na⁺], 2158.2 [Na⁺], 2516.3 [Na⁺] and 2607.6 [Na⁺] corresponded to the proposed structure (Figure 4D). This was also observed in human ions 2447.1, 3257.6, and 3618.8 and pig ions 2621.2, 3431.7 and 3792.8, respectively (Figures 3 and 4). Table 1 summarizes the identified ions for human, domestic, GGTA1 and GGTA1/CMAH pigs with the observed masses and proposed structures shown in Figures 3 and 4. The absence of an ion m/z in Table 1 indicates either an unidentified ion peak or no detection of that ion m/z.

DISCUSSION

Preformed human antibodies directed towards carbohydrate epitopes continue to be a barrier to successful xenotransplantation. The generation of GGTA1/CMAH knock out pigs has reduced but not eliminated the impact of human antibody mediated cytotoxicity *in vitro* (4). In an effort to further reduce human antibody binding in genetically modified pigs, we characterized the serum protein glycome of humans and the pigs we hope will be a solution

to the human organ shortage. Our annotation of the human and pig N-linked glycomes corroborated several previous annotations of cellular and serum proteins (8,9,21,22). The majority of annotated structures provided in Figures 3 and 4 matched those entered in existing databases and many were validated by MALDI-TOF/TOF analysis (not shown). Structures, however, contain positional isomers that could significantly alter the immunoreactivity of a glycan. We made a concerted effort to remain unbiased regarding the genetic modification of the pigs when evaluating positional isomers resulting in perhaps an under-representation of blood groups involving sialylation and/or fucosylation of glycan antennae in contrast to core structures. We did, however, identify ion 2465.2 (hex6,hexNAc4,dhex1) annotated as bearing a terminal gal/gal oligosaccharide, present in humans and domestic pigs but absent in GGTA1 knockout and GGTA1/CMAH knockout pigs (Table 1). This ion may represent alpha or beta linkages other than aGal in humans but inclusive of aGal in pigs. The loss of ion 2465.2 is supported by our previous characterization of the GGTA1 knockout pigs lacking the aGal epitope (23). The existing MALDI-TOF technology has limitations, as the absence of ion 2465.2 in GGTA1 and GGTA1/CMAH pigs cannot be fully attributed to genetic modification without further analysis, such as two-dimensional nuclear magnetic resonance. We also identified several masses in humans that contained neu5Gc and were validated by the presence of mass fragments that could only be possible with the inclusion of the mass representing sodiated and permethylated neu5Gc. This was not surprising since neu5Gc can be incorporated onto human N-linked glycans from dietary sources (24). Further analysis is needed to clarify if dietary incorporation of neu5Gc explains the terminal sialic acid of ions 3012.4 and 3345.6 in pigs. Because we could identify previously described xenoantigens in human and domestic pig mass spectra, we felt confident that the discovery of N-linked glycans more abundant or unique to the GGTA1/CMAH knockout pigs may represent, at least in part, potential targets for further genetic modifications.

Quantitation of unmodified or native glycans by mass spectrometry has proven challenging due to instability and unpredictable fragmentation. Wada and colleagues and more recently Alley and colleagues have improved relative quantitation and fragmentation using protocols to stabilize glycans by reduction and permethylation (9,14). While mass spectrometry of the type used in this study is not fully quantitative we have established a relative quantitation based on the strength of the permethylated glycan ion signal of MALDI-TOF spectra across identically processed samples and/or limited mass range (14). We reduced and permethylated the glycan samples and limited the mass range of analysis in an attempt to provide a relative percent intensity that could be compared between spectra.

Asparagine-linked glycans are produced from a glucosylated high mannose precursor on the inner surface of the endoplasmic reticulum (ER) that is necessary for proper protein folding. This glc3man9glcNAc2 is then de-glucosylated resulting in man9 which we found equally abundant in human and pig samples (25). The N-linked glycan attached to the properly folded protein undergoes glycoprotein specific modification in the lumen of the ER and Golgi controlled by waves of de-glycosylating enzymes such as mannosidase and surges of glycosyltransferases such as alpha 1,3 galactosyl transferase. Failure to make the correct glycosylation changes or maintain correct protein folding, results in shuttling back to the ER or earlier Golgi for re-glycosylation and re-folding. We observed that pig samples with a

mutated GGTA1 or GGTA1 and CMAH genes had higher relative amounts of mannosylated and truncated glycans than human samples. It is difficult to correlate these relative changes to a loss of the GGTA1 enzyme or lack of expression of CMAH enzyme, but we hypothesize that the loss of the GGTA1 enzyme in the glyco-synthetic pathway of the golgi creates a partial barrier to further glycosylation resulting in a pool of incomplete glycans leading to higher mannosylation and exposed terminal N-acetylglucosamines (glcNAc) on core N-linked glycans. This has proven true in genetic modifications of the yeast glycan biosynthetic pathway creating an excess of man5 (26). The accumulation of truncated glycans is also associated with congenital disorders of glycosylation. Patients with a mutation in the ALG9 gene also accumulate high mannose and truncated glycans that affect protein transfer efficiency, the quality control of newly synthesized glycoproteins and can lead to premature degradation of truncated glycoproteins (27). We do not see an obvious pathology in the GGTA1/CMAH knockout pigs that could be related to the symptoms of patients with the ALG-9 defect. In fact, glycan microarray analysis of human antibody binding indicated that recognition of simple mannosylated glycans was on the lowest end of their scale (7). With that said, asymptomatic accumulation of Man3, Man5, Man6, Man7, Man8 and truncated glycans with one or two exposed glcNAc may reduce fecundity and peak function of organ systems. Further studies may show that genetic modification induced incomplete glycan synthesis may require a new strategy for silencing the genes producing already proven xenoantigens such as aGal. One alternative has been to express the human α 1,2 fucosyltransferase gene in pigs to create an environment where gal α 1,3 gal could be fucosylated to become the human blood group H antigen (28,29). Conversion of aGal to the H antigen with concomitant expression of human complement regulatory proteins may inspire new strategies to overcome the accumulation of high mannose and truncated glycans suggested by this study. This approach has proven successful in vitro and in vivo creating cells and organs that are less damaged by antibody-mediated rejection or survive longer after transplantation to non-human primates (28–30). Unfortunately, not all aGal was fucosylated and it is unclear if incomplete production of the H antigen was tissue specific, related to the promoter, or further modified by endogenous expression of fucosidases in the golgi (30). A better understanding of the glycan differences between humans and pigs may lead to additional transgenes as an alternative to knocking out multiple genes.

Xylose in mammals is found on O-linked glycans, in the construction of glycosaminoglycans, heparin and chondroitin sulfate and can occur in the ER, Golgi or serum by xylosyltransferase I and II (31,32). The occurrence of a core linked xylose on mammalian N-linked glycans has yet to be observed which is why we were surprised to identify an N-linked glycan of mass 2245.8 whose fragmentation pattern corresponded to several xylose containing structures (Figure 5). We repeated the glycan isolation protocol, MALDI-TOF and TOF/TOF analyses several times with the same result. It is possible that xylose containing N-linked glycans result from a combination of an abundance of truncated glycans in the presence of a rich source of dietary xylose. There is no evidence that xylosyltransferases are up regulated in pigs but a diet high in plant xylose may create a scenario similar to that of the incorporation of dietary neu5Gc in humans (24). Cultured cells secrete up to 90% of xylosyltransferase activity to the culture media (33). Therefore, if the majority of xylosyltransferase occurs in serum then high concentrations of dietary xylose

may impact xeno-reactivity. The presence of xylose on the ion 2245.8 may elicit human IgG and IgE antibody binding based on studies of plant allergens associated with plant pollen and peanut allergens (34). If pig xylosylation can be verified, it may become important to test individuals for anti-xylose antibodies prior to xenotransplantation. It is hard to imagine immunoreactivity to a glycan that is present in both humans and pigs. This may be explained by antigen density as we have shown in this study (Figure 6), or species-specific modifications to the mannose core where xylose is attached shielding antibody binding (34). Upregulation of xylosyltransferase in humans has been associated with osteoarthritis, systemic sclerosis and nephropathy in type 1 diabetes (33,35,36). The immune-reactivity of xylose on mammalian glycans, concentration and availability of enzyme and substrate need to be verified before further genetic modifications in pigs should be considered.

Similar to beta 1,2 linked xylose, fucosylation can be a target of human antibody when linked alpha 1,3 to a N-linked glycan core glcNAc or as part of disparate blood group antigen (7,37). We identified the most abundant glycan in human samples (2808.3 *m/z*) and all of the pig samples (2982.2 *m/z*) as a bi-antennary complex type glycan with terminal neuAc (Figure 2). The difference in mass was due to a fucosylation of the core glcNAc in all of the pig samples (Figure 5D). The presence of fragments indicative of core fucosylation (490.3 *m/z*) substantiates our proposed structure for this ion but there may be positional isomers that would present the fucose as a terminal blood group or other antennae linkage. As a trend among all samples tested increased fucosylation was the most striking difference between human and pigs but perhaps challenging to address with regard to xenotransplantation. Mice lacking alpha 1,3 fucosyltransferase have a loss of the lewis X structure but have significant psychological changes and may alter the sensory nervous system (38,39).

This study has presented the human and pig serum protein glycomes and in the interest of xenotransplantation, the glycomes of pigs lacking two carbohydrate xenoantigens. Four important observations emerged. The GGTA1/CMAH knockout pigs had more: mannosylated N-linked glycans, incomplete glycan synthesis, xylosylated N-linked glycans, and fucosylation of existing bi- and tri-antennary N-linked glycans. Further studies of the individual glycans are necessary to determine the impact of these carbohydrates on xenotransplantation.

Acknowledgments

The authors thank Dr. Milos Novotny, William Alley and Dr. Rene Ranzinger for their advice and guidance. This work was supported by the Indiana University Health Transplant Institute. Marshall Bern and Alejandro Brito were supported by NIH grant R01 GM103428.

ABBREVIATIONS

AMR	Antibody-mediated rejection
MALDI-TOF	Matrix-assisted laser desorption/ionization time-of-flight
aGal	galactose α -1,3 galactose

neu5Gc	N-glycolyl neuraminic acid
neu5Ac	N-acetyl neuraminic acid
CMAH	cytidine monophosphate-N-acetylneuraminic acid hydroxylase
ER	endoplasmic reticulum
HPLC	high pressure liquid chromatography
ACN	acetonitrile
TFA	trifluoroacetic acid
DMF	N,N-dimethylformamide

References

- Galili U, Macher BA, Buehler J, Shohet SB. Human natural anti- α -galactosyl IgG. II. The specific recognition of α (1---3)-linked galactose residues. *J Exp Med*. 1985 Aug 1; 162(2): 573–82. Internet. Available from: <http://eutils.ncbi.nlm.nih.gov/entrez/eutils/efetch.fcgi?dbfrom=pubmed&id=2410529&retmode=ref&cmd=prlinks>. [PubMed: 2410529]
- Oriol R, Ye Y, Koren E, Cooper DK. Carbohydrate antigens of pig tissues reacting with human natural antibodies as potential targets for hyperacute vascular rejection in pig-to-man organ xenotransplantation. *Transplantation*. 1993 Dec; 56(6):1433–42. Internet. Available from: <http://eutils.ncbi.nlm.nih.gov/entrez/eutils/efetch.fcgi?dbfrom=pubmed&id=8279016&retmode=ref&cmd=prlinks>. [PubMed: 8279016]
- Chen G, Qian H, Starzl T, Sun H, Garcia B, Wang X, et al. Acute rejection is associated with antibodies to non-Gal antigens in baboons using Gal-knockout pig kidneys. *Nat Med*. 2005 Dec; 11(12):1295–8. [PubMed: 16311604]
- Lutz AJ, Li P, Estrada JL, Sidner RA, Chihara RK, Downey SM, et al. Double knockout pigs deficient in N-glycolylneuraminic acid and Galactose α -1,3-Galactose reduce the humoral barrier to xenotransplantation. *Xenotransplantation*. 2013 Feb 5; 20(1):27–35. Internet. Available from: <http://eutils.ncbi.nlm.nih.gov/entrez/eutils/efetch.fcgi?dbfrom=pubmed&id=23384142&retmode=ref&cmd=prlinks>. [PubMed: 23384142]
- Taylor RE, Gregg CJ, Padler-Karavani V, Ghaderi D, Yu H, Huang S, et al. Novel mechanism for the generation of human xeno-autoantibodies against the nonhuman sialic acid N-glycolylneuraminic acid. *J Exp Med*. 2010 Aug 2; 207(8):1637–46. [PubMed: 20624889]
- Basnet NB, Ide K, Tahara H, Tanaka Y, Ohdan H. Deficiency of N-glycolylneuraminic acid and Gal α 1-3Gal β 1-4GlcNAc epitopes in xenogeneic cells attenuates cytotoxicity of human natural antibodies. *Xenotransplantation*. 2010 Dec 16; 17(6):440–8. [PubMed: 21158945]
- Oyeleran O, McShane LM, Dodd L, Gildersleeve JC. Profiling human serum antibodies with a carbohydrate antigen microarray. *J Proteome Res*. 2009 Sep; 8(9):4301–10. [PubMed: 19624168]
- North SJ, Gunten von S, Antonopoulos A, Trollope A, MacGlashan DW, Jang-Lee J, et al. Glycomic analysis of human mast cells, eosinophils and basophils. 2012 Jan; 22(1):12–22. Available from: <http://eutils.ncbi.nlm.nih.gov/entrez/eutils/efetch.fcgi?dbfrom=pubmed&id=21725073&retmode=ref&cmd=prlinks>.
- Alley WR, Vasseur JA, Goetz JA, Svoboda M, Mann BF, Matei DE, et al. N-linked glycan structures and their expressions change in the blood sera of ovarian cancer patients. *J Proteome Res*. 2012 Apr 6; 11(4):2282–300. [PubMed: 22304416]
- Adamczyk B, Tharmalingam T, Rudd PM. Glycans as cancer biomarkers. *Biochim Biophys Acta*. 2012 Sep; 1820(9):1347–53. Internet. Available from: <http://eutils.ncbi.nlm.nih.gov/entrez/eutils/efetch.fcgi?dbfrom=pubmed&id=22178561&retmode=ref&cmd=prlinks>. [PubMed: 22178561]
- Henry HH, Tissot JD, Messerli BB, Markert MM, Muntau AA, Skladal DD, et al. Microheterogeneity of serum glycoproteins and their liver precursors in patients with

carbohydrate-deficient glycoprotein syndrome type I: apparent deficiencies in clusterin and serum amyloid P. *Journal of Laboratory and Clinical Medicine*. 1997 Apr 1; 129(4):412–21. Internet. Available from: <http://www.sciencedirect.com/science/article/pii/S0022214397900743>. [PubMed: 9104884]

12. Triffitt JT, Gebauer U, Ashton BA, Owen ME, Reynolds JJ. Origin of plasma alpha2HS-glycoprotein and its accumulation in bone. *Nature*. 1976 Jul 15; 262(5565):226–7. Internet. Available from: <http://eutils.ncbi.nlm.nih.gov/entrez/eutils/elink.fcgi?dbfrom=pubmed&id=934340&retmode=ref&cmd=prlinks>. [PubMed: 934340]
13. Satomaa, T.; Heiskanen, A.; Mikkola, M.; Olsson, C.; Blomqvist, M.; Tiittanen, M., et al. *BMC Cell Biol*. Vol. 10. BioMed Central Ltd; 2009. The N-glycome of human embryonic stem cells; p. 42. Internet Available from: <http://www.biomedcentral.com/1471-2121/10/42>
14. Wada Y, Azadi P, Costello CE, Dell A, Dwek RA, Geyer H, et al. Comparison of the methods for profiling glycoprotein glycans--HUPO Human Disease Glycomics/Proteome Initiative multi-institutional study. 2007 Jan 12; 17(4):411–22. Available from: <http://www.glycob.oxfordjournals.org/cgi/doi/10.1093/glycob/cwl086>.
15. Mechref Y, Kang P, Novotny MV. Solid-phase permethylation for glycomic analysis. *Methods in molecular biology* (Clifton, NJ). 2009; 534:53–64. Internet. Available from: <http://eutils.ncbi.nlm.nih.gov/entrez/eutils/elink.fcgi?dbfrom=pubmed&id=19277536&retmode=ref&cmd=prlinks>.
16. Ceroni, A.; Maass, K.; Geyer, H.; Geyer, R.; Dell, A.; Haslam, SM. *J Proteome Res*. Vol. 7. American Chemical Society; 2008 Apr. GlycoWorkbench: A Tool for the Computer-Assisted Annotation of Mass Spectra of Glycans †; p. 1650–9. Internet Available from: <http://pubs.acs.org/doi/abs/10.1021/pr7008252>
17. Goldberg D, Sutton-Smith M, Paulson J, Dell A. Automatic annotation of matrix-assisted laser desorption/ionization N-glycan spectra. *Proteomics*. 2005 Mar; 5(4):865–75. Internet. Available from: <http://eutils.ncbi.nlm.nih.gov/entrez/eutils/elink.fcgi?dbfrom=pubmed&id=15693066&retmode=ref&cmd=prlinks>. [PubMed: 15693066]
18. Varki A, Cummings RD, Esko JD, Freeze HH, Stanley P, Marth JD, et al. Symbol nomenclature for glycan representation. *Proteomics*. 2009 Dec; 9(24):5398–9. Internet. Available from: <http://eutils.ncbi.nlm.nih.gov/entrez/eutils/elink.fcgi?dbfrom=pubmed&id=19902428&retmode=ref&cmd=prlinks>. [PubMed: 19902428]
19. Domon, B.; Costello, CE. *Glycoconj J*. Vol. 5. Kluwer Academic Publishers; 1988. A systematic nomenclature for carbohydrate fragmentations in FAB-MS/MS spectra of glycoconjugates; p. 397–409. Internet Available from: <http://link.springer.com/10.1007/BF01049915>
20. Apte A, Meitei NS. Bioinformatics in glycomics: glycan characterization with mass spectrometric data using SimGlycan. *Methods Mol Biol*. 2010; 600:269–81. [PubMed: 19882135]
21. Kim Y-G, Gil G-C, Harvey DJ, Kim B-G. Structural analysis of alpha-Gal and new non-Gal carbohydrate epitopes from specific pathogen-free miniature pig kidney. *Proteomics*. 2008 Jul 1; 8(13):2596–610. [PubMed: 18546155]
22. Kim Y-G, Gil G-C, Jang K-S, Lee S, Kim H-I, Kim J-S, et al. Qualitative and quantitative comparison of N-glycans between pig endothelial and islet cells by high-performance liquid chromatography and mass spectrometry-based strategy. *J Mass Spectrom*. 2009 Jul; 44(7):1087–104. [PubMed: 19373860]
23. Li, P.; Estrada, JL.; Burlak, C.; Tector, AJ. Biallelic knockout of the α -1,3 galactosyltransferase gene in porcine liver-derived cells using zinc finger nucleases. *Journal of Surgical Research* [Internet]. 2012 Jul. Available from: <http://eutils.ncbi.nlm.nih.gov/entrez/eutils/elink.fcgi?dbfrom=pubmed&id=22795272&retmode=ref&cmd=prlinks>
24. Tangvoranuntakul P, Gagneux P, Diaz S, Bardor M, Varki N, Varki A, et al. Human uptake and incorporation of an immunogenic nonhuman dietary sialic acid. *Proc Natl Acad Sci USA*. 2003 Oct 14; 100(21):12045–50. Internet. Available from: <http://eutils.ncbi.nlm.nih.gov/entrez/eutils/elink.fcgi?dbfrom=pubmed&id=14523234&retmode=ref&cmd=prlinks>. [PubMed: 14523234]
25. Parodi AJ. Role of N-oligosaccharide endoplasmic reticulum processing reactions in glycoprotein folding and degradation. *Biochem J*. 2000 May 15; 348(Pt 1):1–13. Internet. Available from: <http://eutils.ncbi.nlm.nih.gov/entrez/eutils/elink.fcgi?dbfrom=pubmed&id=10794707&retmode=ref&cmd=prlinks>. [PubMed: 10794707]

26. Park JN, Lee DJ, Kwon O, Oh DB, Bahn YS, Kang HA. Unraveling Unique Structure and Biosynthesis Pathway of N-Linked Glycans in Human Fungal Pathogen *Cryptococcus neoformans* by Glycomics Analysis. *J Biol Chem*. 2012 Jun 1; 287(23):19501–15. Internet. Available from: <http://eutils.ncbi.nlm.nih.gov/entrez/eutils/elink.fcgi?dbfrom=pubmed&id=22500028&retmode=ref&cmd=prlinks>. [PubMed: 22500028]
27. Vleugels W, Keldermans L, Jaeken J, Butters TD, Michalski JC, Matthijs G, et al. Quality control of glycoproteins bearing truncated glycans in an ALG9-defective (CDG-IL) patient. *Glycobiology*. 2009 Jul 1; 19(8):910–7. Internet. Available from: <http://eutils.ncbi.nlm.nih.gov/entrez/eutils/elink.fcgi?dbfrom=pubmed&id=19451548&retmode=ref&cmd=prlinks>. [PubMed: 19451548]
28. RAMIREZ P. Study of xenograft rejection in a model of liver xenotransplantation from unmodified pig to primate. *Transplant Proc*. 1999 Nov; 31(7):2814–7. [PubMed: 10578302]
29. Costa C, Zhao L, Burton WV, Rosas C, Bondioli KR, Williams BL, et al. Transgenic pigs designed to express human CD59 and H-transferase to avoid humoral xenograft rejection. *Xenotransplantation*. 2002 Jan; 9(1):45–57. [PubMed: 12005104]
30. Costa C, Zhao L, Burton WV, Bondioli KR, Williams BL, Hoagland TA, et al. Expression of the human alpha1,2-fucosyltransferase in transgenic pigs modifies the cell surface carbohydrate phenotype and confers resistance to human serum-mediated cytolysis. *FASEB J*. 1999 Oct; 13(13):1762–73. [PubMed: 10506579]
31. Kuhn, J.; Götting, C.; Schnölzer, M.; Kempf, T.; Brinkmann, T.; Kleesiek, K. First Isolation of Human UDP-d-Xylose: Proteoglycan Core Protein β -d-Xylosyltransferase Secreted from Cultured JAR Choriocarcinoma Cells. 2001. Available from: <http://www.jbc.org/content/276/7/4940.short>
32. Schon S. Cloning and Recombinant Expression of Active Full-length Xylosyltransferase I (XT-I) and Characterization of Subcellular Localization of XT-I and XT-II. *J Biol Chem*. 2006 Feb 17; 281(20):14224–31. Internet. Available from: <http://www.jbc.org/cgi/doi/10.1074/jbc.M510690200>. [PubMed: 16569644]
33. Götting C, Kuhn J, Sollberg S, Huerkamp C, Brinkmann T, Krieg T, et al. Elevated serum xylosyltransferase activity correlates with a high level of hyaluronate in patients with systemic sclerosis. *Acta dermato-venereologica*. 2000 Jan; 80(1):60–1. Internet. Available from: <http://eutils.ncbi.nlm.nih.gov/entrez/eutils/elink.fcgi?dbfrom=pubmed&id=10721843&retmode=ref&cmd=prlinks>. [PubMed: 10721843]
34. van Ree R, Cabanes-Macheteau M, Akkerdaas J, Milazzo J-P, Loutelier-Bourhis C, Rayon C, et al. beta (1,2)-Xylose and alpha (1,3)-Fucose Residues Have a Strong Contribution in IgE Binding to Plant Glycoallergens. 2000 Apr 6; 275(15):11451–8. Available from: <http://www.jbc.org/cgi/doi/10.1074/jbc.275.15.11451>.
35. Schön S, Prante C, Müller S, Schöttler M, Tarnow L, Kuhn J, et al. Impact of polymorphisms in the genes encoding xylosyltransferase I and a homologue in type 1 diabetic patients with and without nephropathy. *Kidney Int*. 2005 Oct; 68(4):1483–90. Internet. Available from: <http://eutils.ncbi.nlm.nih.gov/entrez/eutils/elink.fcgi?dbfrom=pubmed&id=16164625&retmode=ref&cmd=prlinks>. [PubMed: 16164625]
36. Schon S, Huep G, Prante C, Müller S, Christ R, Hagena F-W, et al. Mutational and functional analyses of xylosyltransferases and their implication in osteoarthritis. *Osteoarthritis and cartilage/OARS, Osteoarthritis Research Society*. 2006 May; 14(5):442–8. Internet. Available from: <http://eutils.ncbi.nlm.nih.gov/entrez/eutils/elink.fcgi?dbfrom=pubmed&id=16376579&retmode=ref&cmd=prlinks>.
37. Wilson IB, Harthill JE, Mullin NP, Ashford DA, Altmann F. Core alpha1,3-fucose is a key part of the epitope recognized by antibodies reacting against plant N-linked oligosaccharides and is present in a wide variety of plant extracts. *Glycobiology*. 1998 Jul; 8(7):651–61. Internet. Available from: <http://eutils.ncbi.nlm.nih.gov/entrez/eutils/elink.fcgi?dbfrom=pubmed&id=9621106&retmode=ref&cmd=prlinks>. [PubMed: 9621106]
38. Kudo T, Fujii T, Ikegami S, Inokuchi K, Takayama Y, Ikehara Y, et al. Mice lacking alpha1,3-fucosyltransferase IX demonstrate disappearance of Lewis x structure in brain and increased anxiety-like behaviors. *Glycobiology*. 2007 Jan; 17(1):1–9. Internet. Available from: <http://eutils.ncbi.nlm.nih.gov/entrez/eutils/elink.fcgi?dbfrom=pubmed&id=16973732&retmode=ref&cmd=prlinks>. [PubMed: 16973732]

39. John, JS.; Claxton, C.; Robinson, MW.; Yamamoto, F. ScienceDirect.com. Developmental Biology - Genetic manipulation of blood group carbohydrates alters development and pathfinding of primary sensory axons of the olfactory systems. Developmental. 2006. InternetAvailable from: <http://www.sciencedirect.com/science/article/pii/S0012160606009778>

Author Manuscript

Author Manuscript

Author Manuscript

Author Manuscript

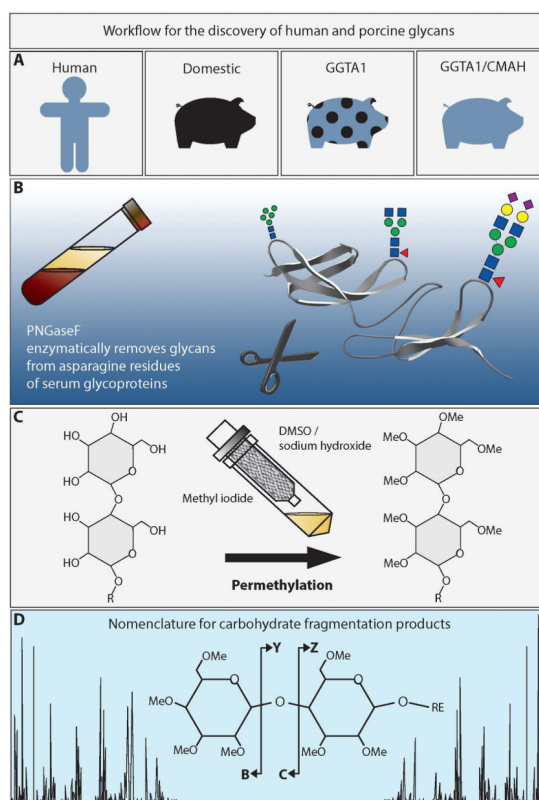


Figure 1. Workflow for the discovery of human and porcine glycans

A. This study compares the N-linked glycomics of humans, domestic pigs, GGTA1 knockout pigs and GGTA1/CMAH knockout pigs. B. Serum samples were treated with the deglycosylating enzyme, PNGaseF, to remove N-linked glycans from serum proteins. C. Native glycans were stabilized by reduction and permethylation on solid-phase sodium hydroxide spin columns. D. Collision induced dissociation of permethylated glycans resulted in predictable fragmentation that was analyzed using the nomenclature of Domon and Costello (19).

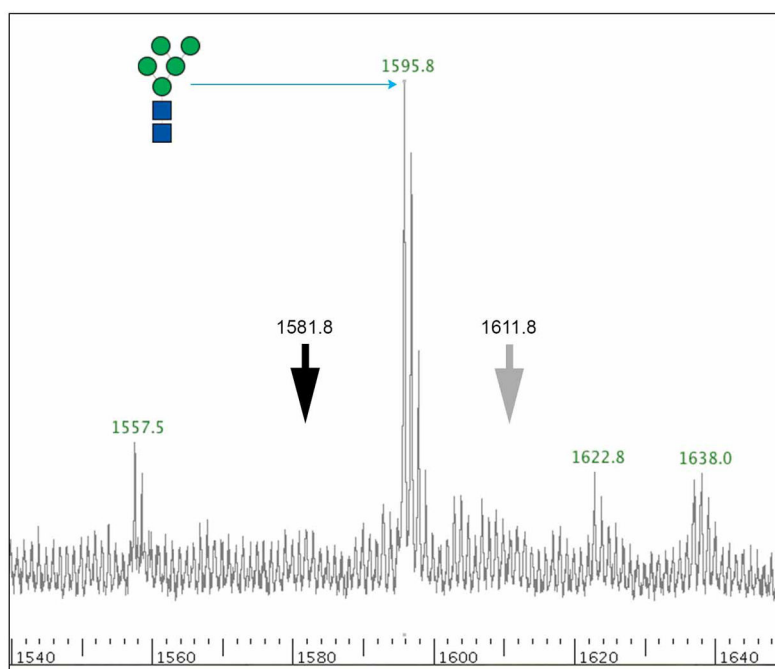
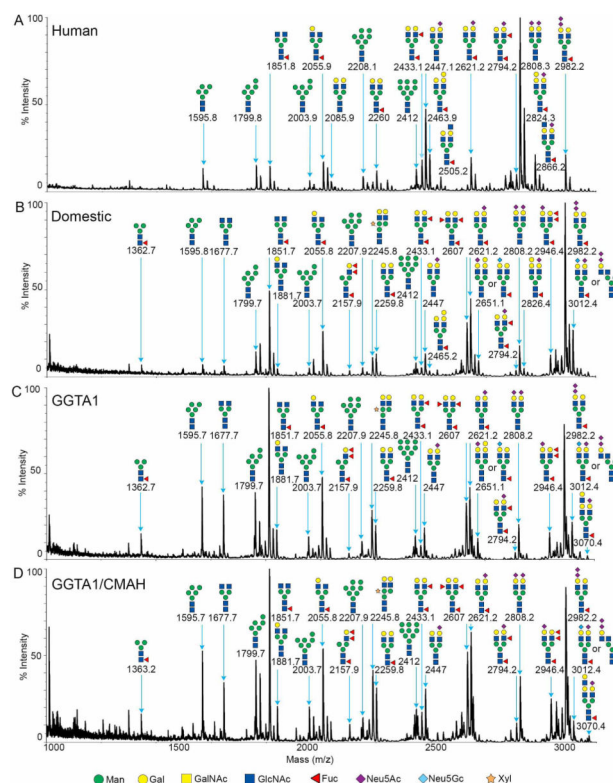


Figure 2.

MALDI-TOF MS profile of ion 1595.8, Man5. Incomplete permethylation results in predictable ions 14 Da downstream of a fully permethylated ion. The black arrow points to the absence of ion 1581.8 m/z , -14 Da from ion 1595.8 m/z . The grey arrow indicates the absence of ion 1611.8 m/z , a +16 Da ion that could originate from the formation of a potassium adduct instead of the more common sodium adduct.

**Figure 3.**

MALDI-TOF MS profiles of the permethylated N-linked glycans from human (A), domestic pigs (B), GGTA1 knockout pigs (C) and GGTA1/CMAH knockout pigs in the range of 1000 to 3100 m/z. Major peaks are annotated with their proposed carbohydrate structures using the nomenclature proposed by the consortium for functional glycomics (18).

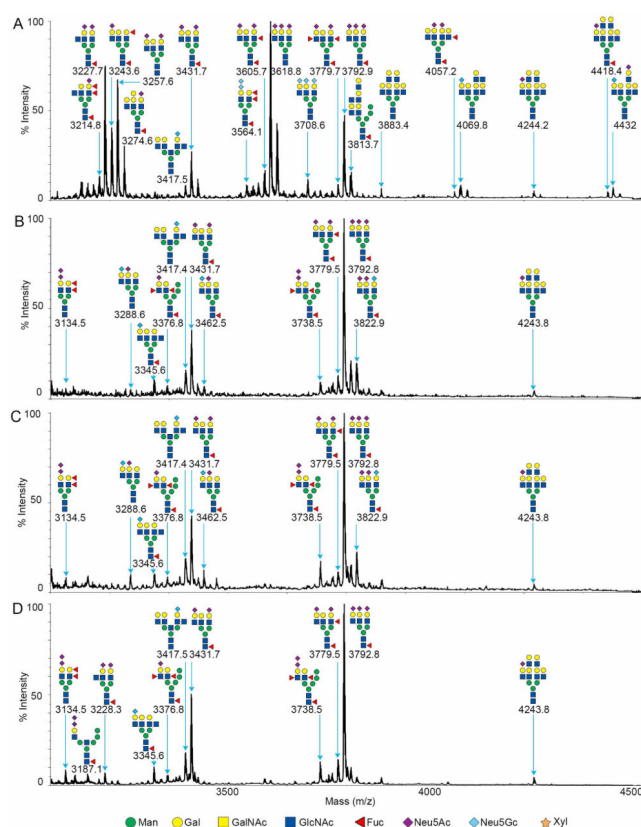


Figure 4. MALDI-TOF MS profiles of the permethylated N-linked glycans from human (A), domestic pigs (B), GGTA1 knockout pigs (C) and GGTA1/CMAH knockout pigs in the ion range of 3100 to 4500 m/z. Major peaks are annotated with their proposed carbohydrate structures using the nomenclature proposed by the consortium for functional glycomics (18).

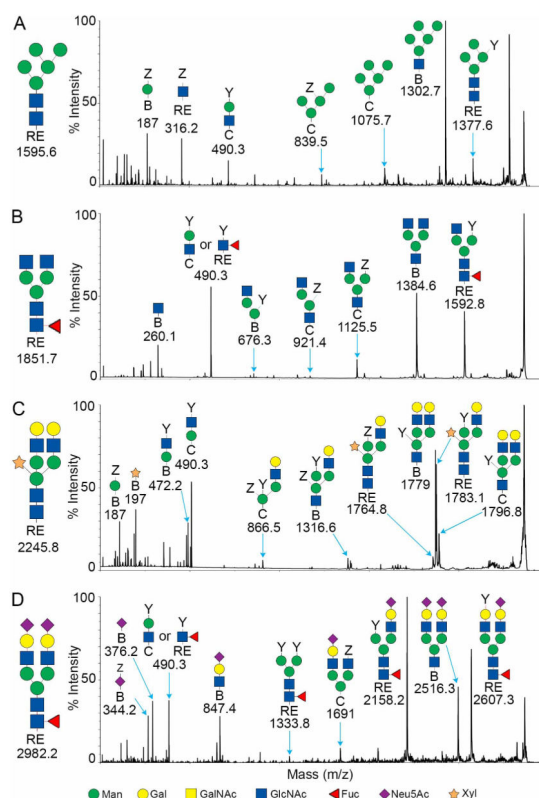


Figure 5.

MALDI-TOF/TOF MS fragmentation profiles for the reduced and permethylated N-linked glycans of the GGTA1/CMAH knockout pig. The ions 1595.7 (A), 1851.8 (B), 2245.8 (C) and 2982.2 (D) were more abundant in the GGTA1/CMAH knockout pigs samples. Major peaks were annotated with their proposed structures based on the proposed carbohydrate structures using the nomenclature of the Consortium for Functional Glycomics (18). The complete N-linked glycan structure is shown to the left of the MS spectra.

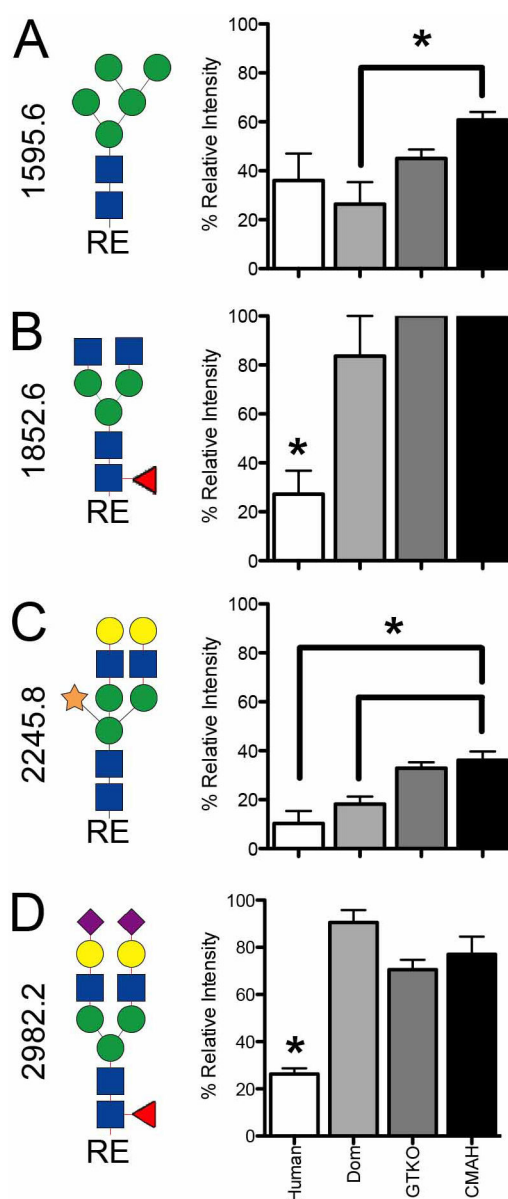



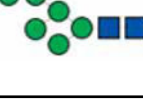



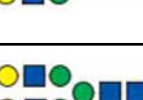

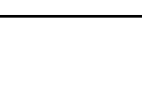





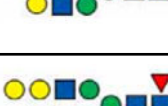
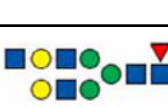
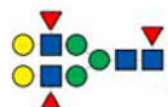
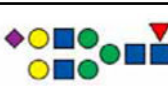
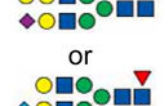
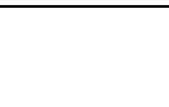















Figure 6. MALDI-TOF/TOF MS fragmentation of N-linked glycans at 1595.7 (A), 1851.8 (B), 2245.8 (C) and 2982.2 (D) were compared between human, domestic pigs, GGTA1 knockout pigs, and GGTA1/CMAH knockout pigs as the percent of relative intensity (n=3). Statistically significant differences were indicated with an asterisk ($P < 0.05$, paired one tailed T-test). Complete structures as determined from MALDI-TOF/TOF analysis are shown to the left of each panel.


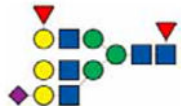


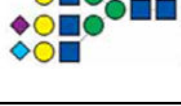

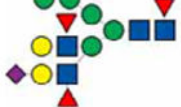


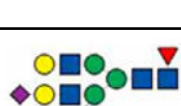
Table 1


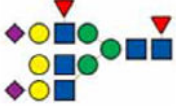

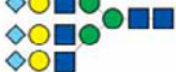
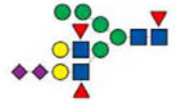
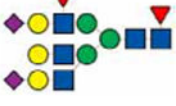




N-linked glycans detected in this study. The observed masses for human, domestic, GGTA1 and GGTA1/CMAH pig serum N-linked glycans are listed by ascending ion m/z.

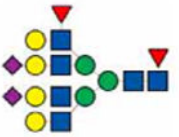




	Human	Domestic	GGTA1	CMAH/GGTA1
		1362.7	1362.7	1363.2
	1595.8	1595.8	1595.7	1595.7
		1677.7	1677.7	1677.7
	1799.8	1799.7	1799.7	1799.7
	1851.8	1851.7	1851.7	1851.7
		1881.7	1881.7	1881.7
	2003.9	2003.7	2003.7	2003.7
	2055.9	2055.8	2055.8	2055.8
	2085.9			
		2157.9	2157.9	2157.9

	Human	Domestic	GGTA1	CMAH/GGTA1
	2208.1	2207.9	2207.9	2207.9
		2245.8	2245.8	2245.8
	2260	2259.8	2259.8	2259.8
	2412	2412	2412	2412
	2433.1	2433.1	2433.1	2433.1
	2447.1	2447	2447	2447
	2463.9	2465.2		
	2505.2			
		2607	2607	2607
		2621.2	2621.2	2621.2
 or 		2651.1	2651.1	

	Human	Domestic	GGTA1	CMAH/GGTA1
	2794.2	2794.2	2794.2	2794.2
	2808.3	2808.2		
	2824.3	2826.4		
	2866.2			
		2946.4	2946.4	2946.4
	2982.2	2982.2	2982.2	2982.2
 or 		3012.4	3012.4	3012.4
			3070.4	3070.4
		3134.5	3134.5	3134.5
				3187.1
	3214.8			

	Human	Domestic	GGTA1	CMAH/GGTA1
	3227.7			3228.3
	3243.6			
	3257.6			
	3274.6			
		3288.6	3288.6	
		3345.6	3345.6	3345.6
		3376.8	3376.8	3376.8
	3417.5	3417.4	3417.4	3417.5
	3431.7	3431.7	3431.7	3431.7
		3462.5	3462.5	

	Human	Domestic	GGTA1	CMAH/GGTA1
	3564.1			
	3605.7			
	3618.8			
	3708.6			
		3738.5	3738.5	3738.5
	3779.7	3779.5	3779.5	3779.5
	3792.9	3792.8	3792.8	3792.8
	3813.7			
		3822.9	3822.9	
	3883.4			

	Human	Domestic	GGTA1	CMAH/GGTA1
	4057.4			
	4069.8			
	4244.2	4243.8	4243.8	4243.8
	4418.4			
	4432			